

Redirection Controller Using Reinforcement Learning

YUCHEN CHANG¹, KEIGO MATSUMOTO¹, (Student member, IEEE), TAKUJI NARUMI¹, (Member, IEEE), TOMOHIRO TANIKAWA¹, (Member, IEEE), MICHITAKA HIROSE¹, (Member, IEEE)

¹The University of Tokyo, Tokyo, 113-0033 JAPAN (e-mail: chang, matsumoto, narumi, tani, hirose@cyber.t.u-tokyo.ac.jp)

Corresponding author: Keigo Matsumoto (e-mail: matsumoto@cyber.t.u-tokyo.ac.jp).

Y. Chang and K. Matsumoto were equally contributed to this paper. The two authors are in alphabetical order.

This work was supported in part by the KAKENHI JP19H04149, JP18J21379

ABSTRACT In the redirected walking fields, there is a high demand for planning the redirected walking techniques and applying them to physical environments with obstacles. Such techniques are mainly managed using three kinds of methods: direct scripting, generalized controller, and physical- or virtual-environment analysis to determine user redirection. The first approach is effective when a user's path and both physical and virtual environments are fixed; however, it is difficult to handle irregular movements and reuse other environments. The second approach has the potential of reusing any environment but is less optimized. The last approach is the most expected and highly versatile but has still not been developed enough. In this study, we propose a novel redirection controller using reinforcement learning, which has advanced plannability/versatility. Our simulation experiments showed that the proposed strategy can reduce the number of resets by 20.3% for physical-space conditions with multiple obstacles.

INDEX TERMS Virtual reality, Redirected walking, Reinforcement learning.

I. INTRODUCTION

WITH the increasing popularity of virtual reality (VR) technologies, such as a head-mounted display (HMD), there is a growing trend in exhibitions where users can walk around freely in immersive virtual environments (IVEs). To walk through a virtual environment (VE), many methods have been proposed and applied so far. One of them involves tracking the user's position and reflecting it onto his/her virtual position in a VE. However, to replicate IVEs through such a system, an equally large physical space is required.

To overcome this problem, redirected walking (redirection) was proposed, which compresses a large VE into a real room, which could be significantly smaller while maintaining the sense of real walking [1]. Numerous redirection techniques have been proposed so far such as rotation, translation, and curvature gains. However, it is next to impossible to freely walk around a VE by using only these individual methods.

Therefore, *redirection controllers* that apply optimal redirection methods at optimal timing have been proposed. Redirection controllers are classified roughly into three types:

scripted, generalized, and predictive controllers [2]. *Scripted controllers* are used for corresponding tracked space with VR space, as determined by the developer in advance. Although this method is most effective when a user walks along a predetermined route, it cannot deal with unexpected movements. *Generalized controllers* guide a user's walking route to specific patterns in a physical space. Although both these methods are highly versatile and adaptive to various walking paths, the optimal method is known to differ depending on the spatial arrangement of VEs [3], [4]. *Predictive controllers* are used for analyzing the tracked space and VE and predicting the walking path of the user to perform appropriate redirection operation at the appropriate time. Much research has been conducted to analyze the spatial composition of a VE and plan effective redirection techniques [5], [6]. However, these methods were not developed adequately for practical use. In particular, there is a need for new methods of coping with cases the presence of obstacles in a physical space.

Meanwhile, recent studies have encouraged the possibility of applying reinforcement learning (RL) to many fields, such as board games [7], robotics [8], and autonomous car [9], by the development of deep learning in recent years. Thus,

it would be natural to try to use deep RL (DRL) to control redirection.

Therefore, in this study, we attempted to construct a novel generalized redirection controller by using RL. It is expected that this novel controller will be able to cope with an environment with obstacles, without the need for individual adjustment. The contributions of this work are as follows:

- 1) Optimization and implementation of a conventional general purpose controller for an environment with obstacles
- 2) Proposal and implementation of a novel generalized redirection controller using RL
- 3) Evaluation of the conventional generalized controller and the RL-based redirection controller in the physical space with obstacles
- 4) Evaluation of a conventional generalized controller and the RL-based redirection controller in different types of walking paths in VE

The remainder of this paper is organized as follows. In Section 2, we review literature related to redirection and RL. Section 3 describes our new redirection controller using RL. Section 4 describes common algorithms and simulation framework of the experiments conducted in this study. In Section 5, we propose and evaluate a heuristic redirection controller for a physical space with obstacles as a preliminary experiment. Section 6 discusses the and evaluation of operations targeted by the redirection controllers using RL. Sections 7 and 8 present the comparisons of the heuristic redirection controller with the redirection controllers using RL in the physical space with obstacles and in different types of VEs. Section 9 presents generalized discussions of this work. Finally, Section 10 summarizes the contributions of this work and presents future enhancements.

II. RELATED WORK

In this section, we introduce relevant research on the redirection method, control of redirection, and DRL.

A. APPROACHES TO REDIRECTED WALKING

Redirected walking (redirection) is a methodology used for walking a vast VE within a limited tracked space, was first proposal by Razzaque [1], and since then, many redirection techniques have been proposed.

A recent survey on redirection provides a comprehensive overview of work in this area [2]. Suma et al. [10] attempted to classify redirection techniques from multiple viewpoints. One of these classifications involves dividing these techniques into subtle or overt manipulations. The advantage of subtle manipulations is that the user does not realize that she/he is being manipulated, and does not prevent natural walking. In contrast, overt manipulations are generally more manageable; the user realizes the manipulation, and the immersion decreases. Subtle manipulations include rotation, translation, curvature and bending gains. Rotation gains can be used to change the amount of rotation of the tracked space

and VE when the user rotates on the spot. Translation gains can be used to change the amount of movement of the user in the real and VR spaces. Curvature gains can shift the walking direction by gradually rotating the user during movement; this allows the mapping of a straight walking path in the VE into a circular path in the tracked space. Bending gains can also change the walking direction of the user walking on the curved path in a tracked space by using a method resembling the curvature gains and allows for the mapping of a curved path in the VE to a different curvature in tracked space. The thresholds of these gains are verified through psychophysical experiments. Bruder, et al. [11] evaluated thresholds of rotation gains and found that compared to in the VE, users can be physically turned approximately 30.9% more and 16.2% less. Similarly, Steinicke et al. [12] found that users can physically turn approximately 49% more and 20% less than in virtual rotation. They also found that imperceptible translation gains range from down-scaling by 14% to up-scaling by 26%. Regarding curvature gains, studies have suggested that users can be redirected in VEs along the circumference of circles with radii of 22 m [12], 11.6 m [13], or 6.4 m [13]. Regarding bending gains, Langbehn et al. [14] found that a curvature in the real world with a radii of $r_{real} = 2.5\text{ m}$ and $r_{real} = 1.25\text{ m}$ can be mapped to a virtually to curvatures of radii $r_{virtual} = 10.875\text{ m}$ and $r_{virtual} = 4.0625\text{ m}$, respectively. In some gains, results differ depending on the research; this is assumed to be due to the difference in attributes of participants, experimental procedures, VEs, and equipment used in experiments. Researchers have also reported that the threshold does not change even if the curvature and translation gains are simultaneously applied [13].

Although performing redirection with such subtle operations is ideal, it is unfortunately not realistic. The user must turn to the center of the tracked space by performing the reset operation when reaching near the boundary of the tracked space. Suma et al. [10] classified these operations as overt methods because they interrupt the user's VE experience in some way. Several methods have been proposed for redirecting users to the center of the tracked space have been proposed, and the most promising of which is called the 2:1-Turn method introduced by Williams et al. [15]. In the 2:1-Turn method, a user is instructed to stop and physically turn, and the VE rotates at twice her/his speed. Thus, the user physically turns 180° and is rotated 360° in the VE. Through such an operation, the user can move forward again; however, the feeling of immersion may decrease because one is forced to stop and rotate on the spot [16]. A resolution to this problem is to the display of distractors, such as a sphere and butterfly moving around the user that guides the user to complete the reset operation [16]. However, selecting an appropriate distractor that matches the content in VE may be difficult, and hence this method is not versatile enough. Therefore, these overt operations should be avoided as much as possible.

B. REDIRECTION CONTROLLER

To walk a vast VE freely, the methods introduced in the previous section must be combined at an optimum time. Redirection controllers have been proposed to perform individual methods at the optimum time. Nilsson et al. [2] pointed out that such a redirection controller can be roughly classified into three types.

The first is the scripted controller, which assumes that the user walks on a predetermined walking route. By using redirection techniques in a predetermined place, it is possible to complete the VR experience by using only subtle operations. However, while using scripted controllers, users experience difficulty when deviating from a predetermined course, and redirection techniques must be changed each time the spatial configurations of the tracked space and VE change.

The second redirection controller is a generalized controller. In general, generalized controllers can be applied regardless of the spatial structure of the VE or tracked space, thus retaining high versatility. Various methods such as Steer-to-Center, Steer-to-Multiple-Waypoint, and Steer-to-Orbit have been proposed as generalized controllers [17]. Steer-to-Center is a method to guide users to the center of a tracked space; Steer-to-Multiple-Waypoint is a method to guide users to multiple points; and Steer-to-Orbit is a method of guiding users to a circular walking route whose center is also the center of the tracked space. Some researchers verified the best method for generalized controllers according to the spatial configuration of the VE; they showed that Steer-to-Center is effective in nearly all cases, whereas Steer-to-Orbit is effective live users [3], [4]. However, there is a limit to optimization for specific space configurations, often requiring overt operations such as resetting.

The third controller is the predictive controller, which attempts to perform the optimal redirection operation at the optimal timing by predicting the walking path of the user based on the spatial configuration of the VE and tracked space. Zmuda et al. [5] proposed an algorithm called FORCE as a redirection controller optimized in a constrained environment. Similarly, Nescher et al. [6] presented an algorithm called MPCRed for dynamically choosing appropriate redirection controllers to optimize space and minimize costs. Methods have also been proposed for extracting a walkable route by using a graph or navigation mesh and predicting the walking route of the user to perform a predictive redirection control [18], [19]. Moreover, Chen et al. [20] tried to apply redirection algorithms to irregular shaped and dynamic physical environments. To improve predictive controller accuracy, Zank and Kunz [18] conducted a research to predict where the user goes. More recently, a kind of machine learning technology called LSTM was also applied to redirection [21]. LSTM is an artificial neural network with the ability to process time series data and make predictions based on them. Using LSTM, This system can predict the user's future path and thus give the corresponding manipulation on redirecting.

In this way, although various trials were conducted for the redirection controller, but it is difficult to select an op-

timal strategy when the real space comprises obstacles or has a complicated shape. Therefore, we decided to create a controller that autonomously constructs the optimal strategy when multiple obstacles exist in real space by using RL.

C. DRL

In this subsection, we will briefly explain about RL and methods used in this study.

1) RL

RL [22], [23] is a type of machine learning, often used in the automatically production of a series of actions, such as robot moving and balancing. Instead of using identifying labels, RL uses positive and negative rewards to evaluate output actions, leading to current environmental result. The use of RL is advantageous in that people who use RL do not need to know the optimal actions required toward goal setting. Some common examples that could use RL as a decision provider are trash-finding robots, pole balancing, GO playing, etc. [23]

An RL can often be described as a Markov decision process with a 4-tuple (S , A , P , and R), where $S \in \mathbb{R}^n$ is the observable-state set, $A \in \mathbb{R}^m$ is the possible action set, $P \in [0, 1]$ is the probability for the state to transit from s_t to s_{t+1} owing to action a_t , and $R \in \mathbb{R}$ is the reward received after the transition of state. Policy $\pi_\theta : S \rightarrow A \in \mathbb{R}^m$, is the function that outputs the best action (i.e. the most reward-receivable action) with the current observation of the environment. θ in the policy π_θ implies all parameters in the policy. The learning part of RL could be explained as follows:

- Agent observes the environment as state s_t
- According to s_t and learned policy π_t , the agent outputs action a_t
- The environment changes due to a_t , and give reward r_t is recompensed to agent
- (r_t, s_t, a_t) is recorded into the trajectory memory, and time moves on to $t + 1$; all the aforementioned steps are then repeated until t_{max} is reached
- Agent updates policy π to π^* according to the trajectory

2) Learning Methods

There are two common architectures of RL for resolving the given problem: (1) a value-based method and (2) a policy-based method. These two methods differs in what RL learn.

The value-based method updates the value (i.e., estimated-reward) function as a reference for the policy to decide which action to take. Q learning [24] is a common value-based method, which stores and updates expected future reward, named the Q value, of every state-action tuple. The value function can be written as:

$$V^\pi(s) = \mathbb{E} \left[\sum_{i=1}^T \gamma^{i-1} r_i | s_t = s \right] \quad (1)$$

where $\gamma \in [0, 1]$ is the discount factor, which shows the importance of considering the future reward.

In contrast, the policy-based method directly adjusts the policy parameter θ . If the policy function $\pi(s, a, \theta)$ is differentiable with respect to θ , we can use policy gradient methods [25] can be used to update θ :

$$\theta_{i+1} = \theta_i + \alpha_i \frac{\partial R}{\partial \theta_i}$$

$$\text{where } \frac{\partial R}{\partial \theta_i} = \sum_s P r^\pi(s) \sum_a \frac{\partial \pi(s, a)}{\partial \theta} Q^\pi(s, a) \quad (2)$$

The policy-based method could perform better for a large state or action space (for example, rational number space), as value-based methods must remember all state-action pairs. A famous approach of policy-based method is REINFORCE [26].

Another method exists that combines the two aforementioned methods: the Actor–Critic method [27]. Actor–Critic method consists of two elements: the Actor, which is a policy that controls the output actions, and the Critic, which is a value function that evaluates the expected return and is used to update the actor. In this paper, we used a variation of the Actor–Critic method as our RL architecture.

3) DRL and Proximal Policy Optimization Algorithm

Deep learning has received increasing attention owing to its satisfactory results in several research fields. It is able to create an approximation of complex nonlinear functions by learning from sufficiently large datasets; this characteristic appropriately matches that of RL, as RL is often used in continuous serial action-deciding problems, such as robot feedback control. In particular, DRL is simply ordinary RL with the learning target (i.e., value function or policy) replaced by deep neural networks.

In this study, a well-known architecture of DRL called the asynchronous advantage actor–critic (A3C) method proposed by [28] was used. In the following, we explain the A3C method by breaking it into three parts.

- **Asynchronous**

Multiple agents work independently in separate environments. After t_{max} time-steps or episodes, separate agents will their own trajectory to update the core neural network. The asynchronous feature speeds up DRL, especially when working on a CPU.

- **Advantage term**

The Advantage term is usually used to update the policy network. Advantage shows the amount of benefits that would be obtained when taking actions. In this study, we considered the estimator used by Mnih et al. [28]:

$$\hat{A}_t = \left(\left(\sum_{i=t}^{T-1} \gamma^{i-t} r_i \right) + \gamma^{T-t} V(s_T) \right) - V(s_t), \quad (3)$$

where the first term at the right-hand side represents the estimated value after T time-steps, and the second term represents the current value. In addition, a generalized

advantage estimation (GAE) in proposed by [29] could be written as

$$\hat{A}_t = \sum_{i=t}^{T-1} (\gamma\lambda)^{i-t} \delta_i \quad (4)$$

$$\text{where } \delta_i = r_t + \gamma V(s_{t+1}) - V(s_t) \quad (5)$$

while $\lambda \in [0, 1]$ is an exponentially weighted hyperparameter. Equation (3) would be equal to (4) if $\lambda = 1$, and δ_i is an one-step advantage estimator.

- **Actor–Critic**

The actor–critic part is the same as that previously explained in Section 2.3.2, with one or two deep neural networks receiving state parameters and outputting actions and estimated value.

4) Used Method

To update the neural network part of DRL, a policy gradient method is often used to simulate the policy gradient to perform gradient ascent. In this study, we used a particular policy gradient method called the proximal policy optimization (PPO), which was proposed by [30]. PPO updates the neural network by using the policy loss function (or objective function):

$$L_t^{CLIP}(\theta) = \mathbb{E}_t \left[\min \left(r_t(\theta) \hat{A}_t, \text{clip}(r_t(\theta), 1 - \epsilon, 1 + \epsilon) \hat{A}_t \right) \right] \quad (6)$$

where $r_t(\theta) = \frac{\pi_\theta(a_t|s_t)}{\pi_{\theta_{old}}(a_t|s_t)}$, ϵ is an coefficient that normally ranges 0.1 and 0.3, and A_t is the advantage function. In addition, when the update is too large, clipping part $\text{clip}(r_t(\theta), 1 - \epsilon, 1 + \epsilon)$ has its effect when the update is too large, slows the learning process down but with more stability.

As we are using the A3C method, for which the value function and policy are both use a neural network, we considered the value function when updating the neural network by using the above-mentioned loss. The actual loss function would be written as

$$L_t^{CLIP+VF+S}(\theta) = \mathbb{E}_t \left[L_t^{CLIP}(\theta) - c_1 L_t^{VF}(\theta) + c_2 S[\pi_\theta](s_t) \right] \quad (7)$$

where c_1 and c_2 are coefficients, L_t^{VF} is the square of the advantage term, and S is the entropy bonus for encouraging DRL to explore.

III. REDIRECTION CONTROLLER USING RL

A. CONCEPT

The purpose of this novel redirection controller is to perform optimized redirection techniques for arbitrary VEs and tracked spaces as well as multiusers online. Therefore, the RL is applied to learn the redirection controller, with the aim of minimizing negative rewards corresponding to side effects of each redirection technique. In this study, RL was considered because sufficient teaching data on redirection does not exist.

In addition, learning in RL is performed without any specific measures and by providing only rewards.

We selected curvature, translation, and rotation gains during resetting as objects to be manipulated. As input of RL, we provided the user's position, orientation, and distance to the surrounding obstacles (boundaries and other users) in tracked space. When the target was known, we also provided the distance to the target in the VE as input.

B. OVERVIEW OF REDIRECTION CONTROLLER

We attempted to adjust the values of translation, rotation, and curvature gains through RL. Based on previous research on detection thresholds for redirected walking [12], [13], the translation gains were limited to the range of 0.86–1.26 and the curvature gains were limited to the range of -0.1333 – 0.1333 ($= 1/7.5$) [m^{-1}]. The rotation angle during the reset operation can take an arbitrary value from 0° to 360° . Generally, in the reset operation, the user stops on the spot and applies the rotation gains while rotating 360° in the VE, thereby changing the user-traveling direction in physical space. The rotation angles applied in this study can be realized by setting an appropriate rotation gain from 0.5 to 1. The output is one vector normalized from -1 to 1 . This vector is converted to translation gains, rotation angles at reset, and curvature gains by multiplying appropriate coefficients.

As inputs, we used position, orientation, distance to surrounding obstacles or boundaries in the physical space, and the previous output vector. The position in the tracked space was normalized between -1 and 1 according to half the length of the room, with the center of the room being 0 . Regarding the direction, the angle was normalized between -1 and 1 by dividing by 180° ; here, the normal facing the center of the room was 0° . The distance to the surrounding obstacles was observed every 6° from the user's periphery, as shown Fig.1, and the observed distances were normalized between 0 and 1 according to the length of the diagonal line of the tracking space. The total input data corresponds to 64 vector observations, including two vectors of the x and z coordinates in the tracking space, one vector of the angle of the user with respect to the center of the tracking space, 60 vectors of the distances to obstacles or boundaries, and one vector of previous output.

C. NETWORK ARCHITECTURE AND TRAINING SETTINGS

Fig.2 shows the model of RL used in this experiment. We used PPO [30] of the Unity ML-Agents Toolkit (Beta) [31] ¹ for RL. PPO maximizes a surrogate objective $\mathbb{E}[\rho_t(\theta)A_t]$, where $\rho_t(\theta) = \pi(a_t|s_t; \theta)/\pi(a_t|s_t; \theta_{old})$ is the likelihood ratio of the recorded action between the updated and original policies. In PPO, the shared neural networks are updated in parallel by multiple agents. The ML-agents toolkit was

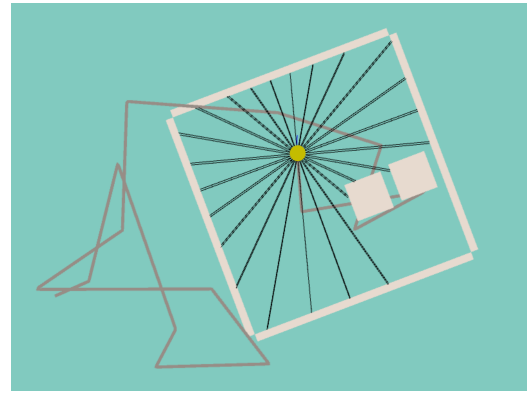


FIGURE 1: Image of training of the RL-based redirection controller. The yellow dots indicate a simulated user (agent). The cream frames and cubes represent the boundary of the tracking space and obstacles, respectively. The gray line represents the 100-m virtual walking path, and the black lines represent the rays measuring the surrounding distance. (In fact, although 60 rays were used, the number was reduced to 24 for better visibility.)

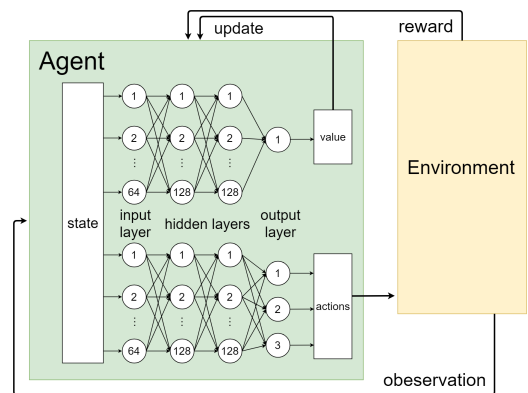


FIGURE 2: Model of proximal policy optimization used in our experiments. Sixteen agents were used during training, and one agent was used during execution.

released by Unity Technologies ² and is run using the Tensorflow ³ background.

We set rewards as shown in Table 1. We normalized curvature gains (g_C) and translation gains (g_T) by using the maximal values of the gain, then squared it and multiplied it by -0.01 . The normalized gain is squared to suppress the sudden change of the gain. We also added a negative reward of changing rate of curvature gains, noted as Δg_C , to further suppress sudden changes. For reset manipulation, we set -45 rewards for each resetting at the boundaries and obstacles. In resetting, the rotation angle was not considered, and the reward was uniformly set. To evaluate whether the current position of the agent is good or bad, we added an additional reward term, named *near obstacle punish*, that cal-

¹<https://github.com/Unity-Technologies/ml-agents>

²<https://unity3d.com/>

³<https://www.tensorflow.org/>

culates the difference between the minimum and maximum distances towards the obstacles or boundary of the tracked space around the agent. Note that the *near obstacle punish* reward increases when the agent nears the center of the tracked space and decreases when the agent is near the boundary or obstacles.

TABLE 1: Rewards of PPO

Parameter	Reward
Curvature gains	$-0.01 * (g_C - 1 /0.1333)^2 - 0.1 * \Delta g_C/0.1333 $
Translation gains	$-0.01 * (g_T - 1 /0.26)^2 - 0.1 * \Delta g_T/0.26 $
Resetting	-45
Near obstacle punish	$0.2 * ((d_{min}/d_{max}) - 1)$

The output normalized from -1 to 1 was multiplied by a coefficient and converted into translation gains, rotation angles, and curvature gains as follows. To set the range of the translation gains within 0.86 and 1.26 , the coefficient for the output of the translation gains was set to 0.2 , and then 1.06 was added. For the rotation angle, the output multiplied by 180 and modulo 360 was used. To set the range of the curvature gains within -0.1333 and 0.1333 , the coefficient for the curvature gains output was set to 0.1333 . Here, the positive and negative values indicate that the curvature is applied in the clockwise and counterclockwise directions, respectively.

The hyperparameter was tuned manually so that the reward would be maximized. Please refer to the appendix for details on hyperparameters.

As a characteristic of PPO, it is possible to learn in parallel using multiple agents. Thus, we used 16 agents for learning, and the total simulation steps were 16 million.

In RL, the learning time is generally inversely proportional to the CPU performance. By using a PC equipped with an Intel Core i7-8750H CPU, the learning time of these models was approximately 2 h. Additionally, the online execution time of the network was approximately 0.301 ms per frame, which is only 1.81% of the duration of a frame in a 60 frames-per-second environment. This execution time is less enough to run the trained agent in practical VR contents with very low overhead.

IV. ENVIRONMENT SETUPS

This section explicates common algorithms and the simulation frameworks of the experiments. (The framework was used in experiments unless otherwise noted).

A. TRACKED SPACE

In this study, the tracked space is a square room with dimensions of $15\text{ m} \times 15\text{ m}$. In experiments using obstacles, each obstacle was set as a cube with a side length of 2.5 m . The obstacles were placed at random positions, and in case of multiple obstacles, it is possible for the obstacles to overlap. In addition, the position of the obstacles was changed every 1000 frames, that is, every 100-m walk of the simulated user.

During the journey, the agent can move freely in the tracked space. However, whenever the agent collides with walls or obstacles, the journey is interrupted and a reset procedure will be performed, in order to orient the agent.

B. WALKING AGENT

To evaluate the performance of the proposed algorithms, a walking agent was designed to simulate how a human would walk in a virtual space. At the start of the journey, a random target destination in the virtual environment is generated, and the agent selects the shortest path toward the target as its walking path. In each simulation step, the agent will first moved 0.1 m along the walking path, and then new values of curvature and translation gains were applied according to the movement result. After the agent has reached its target, the next target was generated immediately to create a continuous journey. In all the following experiments of RL, we used 16 agents in parallel environments while training, and one agent while evaluating.

C. VIRTUAL PATH GENERATION

To allow the agents to continue moving, a new target was generated in the VE would be generated whenever a user reached the current target. We used a procedural random path generator in order to make the agent continue moving during the journey. When generating a new target, we take the user's current position and proceeding direction as references, and set the target position according to different methods introduced in [32], [33] (see table 2), where $unif(a, b)$ is a random value from uniform distribution between a and b , and $Random$ is a combination of *Exploration small* and *Exploration large*.

TABLE 2: path generating methods

Category	Distance [m]	Direction [rad]
Office Building	$unif(2, 8)$	$\{-\frac{\pi}{2}, \frac{\pi}{2}\}$
Exploration (small)	$unif(2, 6)$	$unif(-\pi, \pi)$
Exploration (large)	$unif(8, 12)$	$unif(-\pi, \pi)$
Long Walk	$\{1000\}$	$unif(-\pi, \pi)$
Random	$unif(2, 12)$	$unif(-\pi, \pi)$

The maximal length of a journey is 100 km (one million simulation steps.) After the maximal length is reached, the agent terminates his journey, and no new target is generated.

V. PRELIMINARY EXPERIMENT: HEURISTIC REDIRECTION CONTROLLER FOR OBSTACLE-BASED ENVIRONMENT

Before testing the RL-based redirection controller, we investigated which combination of generalized controllers gives the best result in a multi-obstacle environment.

A. HEURISTIC ALGORITHMS

1) Translation Gains

- Center-based Translation Gain

The *center-based translation gain (CTG)*, proposed by [32], works as follows:

$$g_T = \begin{cases} 1.26 & , \text{if } v_{center} \cdot v_{targ} < 0 \\ 1 & , \text{else} \end{cases} \quad (8)$$

where v_{center} and v_{targ} are vectors pointing toward the center of the tracked space and current user proceeding direction, respectively. The main idea of CTG is to slow down the user when the user is moving away from the center of the tracked space.

- Advanced CTGs

We proposed the *Advanced CTG (ACTG)* algorithm, which is similar to CTG. When the agent is moving away from the center of the tracked space, larger translation gains would be applied to slow down the agent; similarly, smaller translation gains would be applied when a user is heading toward the center of the tracked space. The unnoticeable minimum and maximum thresholds of translation gains were selected as 0.86 to 1.26, respectively, as introduced in [34]. The output translation gain was then calculated as follows:

$$g_T = 1.06 - 0.2 \cos(\alpha_{center}) \quad (9)$$

where α_{center} is the angle between the target direction and the direction toward room center, ranging in $(-\pi, \pi)$. This provides a smooth change in the translation gains when the user is changing direction.

2) Reset Algorithms

- Turn-to-Center

The 2:1-Turn is the most commonly used form of the reset, and it performs a 180° turn in reality, which in the VE is a 360° turn in the VE [15]. However, as reported by Nguyen et al. [35], by using this method, the simulated user may go back and forth in the corners of the tracked space for a long time. To overcome this problem, Peck et al. [36] directed the user to the center of the tracked space at reset. In addition, Nguyen et al. [35] proposed a method to direct the user to the corner farthest away from the user's position. They named these methods as to-center and to-corner, respectively [35]. As to-center may be mistaken for Steer-to-Center (S2C), we henceforth refer to to-center from now on as *Turn-to-Center (T2C)*.

- Turn-to-Furthest

In addition to T2C and to-corner, we proposed a new reset method called *Turn-to-Furthest (T2F)*. Similar to to-corner, T2F will force the user to face the furthest straight route she/he can walk in her/his current position. As T2F considered the shape of the tracked space and agent's current position into account, it is expected to perform better than T2C and to-corner when there are random obstacles in the tracked space.

3) Curvature Gains Algorithms

- S2C

S2C was chosen as the curvature gains algorithm because of its effectiveness in a generalized environment [3]. S2C

simply steers the user to face the center of the tracked space by considering the center as most likely being the farthest place from walls and obstacles. We used the algorithm introduced in [37], which is a modification of Razzaque's original algorithm [1] but more dynamic and versatile.

B. SIMULATION SETUP

We compared four different combinations of the heuristic controllers: the translation gain algorithm was chosen from CTG or ACTG, the reset algorithm was chosen from T2C or T2F, and the S2C was selected as the curvature gains algorithm. We ran each controller in a 100-km journey (one million simulation steps) with 0-3 obstacles. Random path generation was used for the walking path in the virtual space, and we used the count of reset procedure as the evaluation criteria.

C. RESULTS

Fig. 3 shows the number of resets in the each heuristic conditions with obstacles. As shown, the number of resets increases when the number of obstacles increases in all methods, as the reset count becomes two times that when three obstacles are placed. No large difference was observed in zero-obstacle condition; however, in the three-obstacles condition, the methods using T2F performed 20.5% (CTG), 26.8% (ACTG) better than those using T2C. Among the four conditions, the method with the least number of resets in any physical environment was that using ACTG, T2F, and S2C. Henceforth, the heuristic condition is referred to by (ACTG, T2F, S2C).

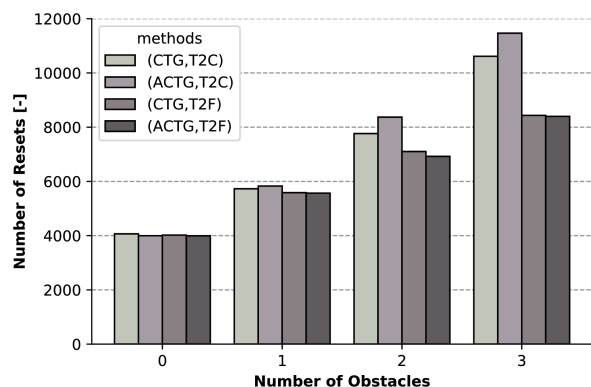


FIGURE 3: Number of resets under the multiple obstacle environment

D. DISCUSSION

We found that adopting T2F as a reset algorithm in obstacle-based environments reduces the number of resets more than when using T2C. This could be because T2C cannot avoid obstacles near the center of the physical space, while T2F finds the furthest point to turn, other than the center.

In addition, the comparison of (CTG, T2F) and (ACTG, T2F) showed that the combination of (ACTG, T2F) showed a smaller number of resets in all environments. Therefore, the most effective conventional generalized controller is that using the combination of (ACTG, T2F, S2C). Hereafter, this controller is called a heuristic controller and will be compared with other controllers using RL.

VI. EXPERIMENT 1: REINFORCEMENT LEARNING FOR TRANSLATION, ROTATION, CURVATURE GAINS

To evaluate the effectiveness of RL, we replaced translation gains, reset angles, and curvature gains algorithm in the heuristic algorithm combination with RL individually. We trained and tested the training result against the heuristic algorithm combination.

A. SIMULATION SETUP

We ran each algorithm combination in a 100-km journey (one million simulation steps) for training and evaluation by using random path generation, and recorded the total count of resets. No obstacle was placed in the tracked place.

Table 3 shows the algorithm used for each redirection controller. The Heuristic controller uses (S2C, T2F, ACTG), which is the best result in the preliminary experiment. RL-prefixed controllers replace one of the curvature, translation, reset algorithms from heuristic with RL, respectively.

TABLE 3: Used Algorithm

	Translation	Reset	Curvature
Heuristic	ACTG	T2F	S2C
RL-translation	RL	T2F	S2C
RL-reset	ACTG	RL	S2C
RL-curvature	ACTG	T2F	RL

B. RESULTS

Table 4 shows the number of resets in the heuristic condition, RL-curvature condition, RL-reset condition, and RL-translation condition. RL-reset and RL-translation conditions are slightly less effective compared with the heuristic condition, although RL-curvature condition has almost the same number of resets as that in the heuristic condition.

TABLE 4: Number of Resets in Experiment 1

Controller	Number of Reset
Heuristic	3994
RL-curvature	3996
RL-reset	4226
RL-translation	4152

Fig. 4 shows the walking paths of the initial 100 m when using the heuristic and RL-curvature controllers. As shown, the RL-curvature controller showed a behavior similar to those of the S2C and Steer-to-Orbit.

Fig. 5 shows the translation gains when a simulated user is walking the initial 100 m in the physical space. In Heuristic, partial-RL-reset, and partial RL curvature algorithms, translation gains changed discontinuously, while in the partial-RL-translation algorithm, translation gains oscillated but

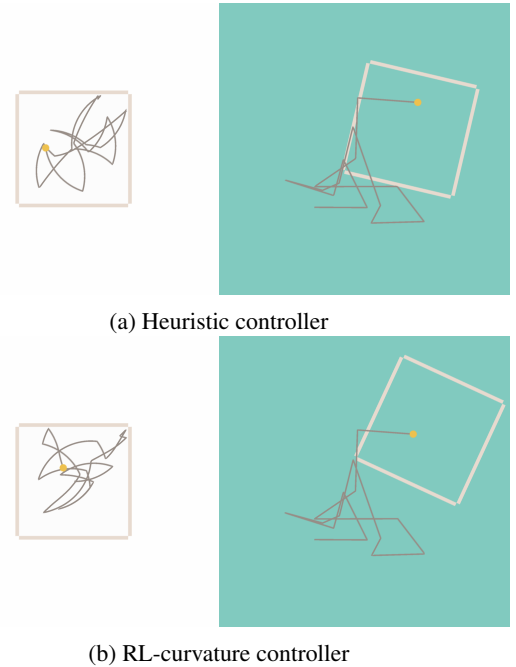


FIGURE 4: The walking path of the initial 100 m when using the heuristic and RL-curvature controllers. The left-hand side shows the physical space and the right-hand side shows the virtual space. The yellow dots indicate simulated users (agents). The cream frames represent the boundary of the tracking space, and the gray lines represent the 100 m physical and virtual walking paths, respectively.

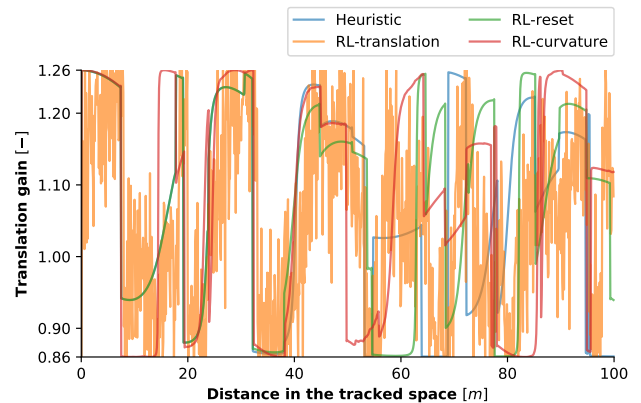


FIGURE 5: Translation gains when a simulated user is walking the initial 100 m in the physical space.

changed continuously. The same pattern was observed in the initial 100 m and beyond.

Fig. 6 shows the average reset angles when a simulated user is walking 100 km in the physical space. The error bars indicate standard variance. In Heuristic, RL-translation, and RL-curvature algorithms, the average reset angles were approximately 180°, while in the RL-reset algorithm, the average reset angle was below 180° and had a greater variance

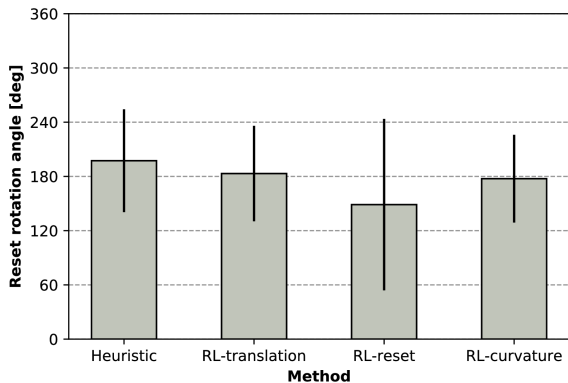


FIGURE 6: Average and standard deviation of reset angles ($mean \pm SD$)

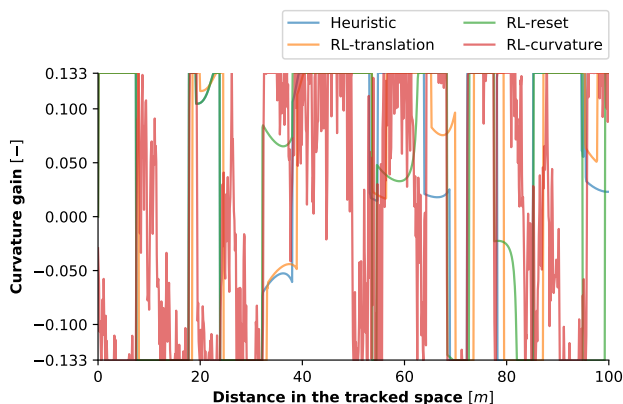


FIGURE 7: Curvature gains when a simulated user is walking the initial 100 m in the physical space.

than the other algorithms.

Fig. 7 shows the curvature gains when a simulated user is walking the initial 100 m in the physical space. In Heuristic, partial RL-translation, and partial RL-reset algorithms, the curvature gains change discontinuously, while in the partial RL-curvature algorithm, the curvature gains oscillated but changed continuously. The same pattern was observed in the initial 100 m and beyond.

C. DISCUSSION

In the unobstructed environment, the number of resets is smaller for the heuristic controller than for the RL-translation and RL-reset controllers. In contrast, the number of resets is almost the same between the heuristic condition in which RL is applied to the curvature gain.

When we applied RL to translation gains and curvature gains, the output gains oscillated. The application of such a sudden change in gains to an actual user may cause awareness of operations and VR sickness to the user. In contrast, when the RL-curvature controller was applied, the walking path in the physical space was smooth and did not show any zigzag.

Hereinafter, among the controllers using RL, the RL curvature controller with the smallest number of resets is called an *RL controller*.

VII. EXPERIMENT 2: RL-BASED REDIRECTION CONTROLLER FOR OBSTACLE-BASED ENVIRONMENTS

Often there are various obstacles in a physical space. For example, furniture, such as tables and pillars, can be considered as obstacles. These obstacles can have a significant impact on the redirection controller, as shown in section 5. In this section, we compare the heuristic redirection controller and the redirection controller using RL in the physical space with obstacles.

A. SIMULATION SETUP

To verify the versatility of the RL-trained redirection controllers in these environments, we placed obstacles into the tracked space and tested their results. We compared the three conditions of the heuristic controller (heuristic), the RL redirection controller trained in the experiment 1 (non-retrain), and the RL redirection controller retrained in the environment with obstacles (retrain). In the trained model, the controller trained in the physical environment without obstacles was used to evaluate the behavior in the physical environment with n obstacles. In the retraining model, the controller trained in the physical environment with n obstacles was used to evaluate the behavior in the physical environment with n obstacles.

We ran each algorithm together in a 100-km journey (one million simulation steps) for training and evaluation by using the random path generation, and recorded the total count of resets in the evaluation.

B. RESULTS

Fig 8 shows the total count of resets in the heuristic, non-retrain RL, retrain RL conditions. One can observe that though the performances of the three controllers are almost the same when there were no obstacles, the performances differed a lot from each other when obstacles were added. When using the heuristic controller, the number of resets increased by 39.4%, 73.4%, and 110%, respectively, with increase in the number of obstacles increased compared to when there were no obstacles. When using the RL controller trained in Experiment 1, the increase in the number of resets of non-retrain RL controller compared to no obstacles environment was 33.9%, 60.3%, and 91.7%, respectively, and the increase in the number of resets of the retrain RL controller was 23.3%, 46.6%, 67.4%, respectively.

When an obstacle exists, compared to a heuristic controller, the RL controller performs better both in the non-retrain model in the experiment 1, and the retrain model in each environment with each path-generating method.

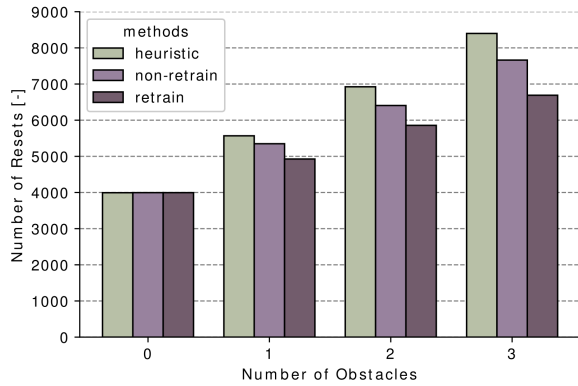


FIGURE 8: Number of resets in Experiment 2

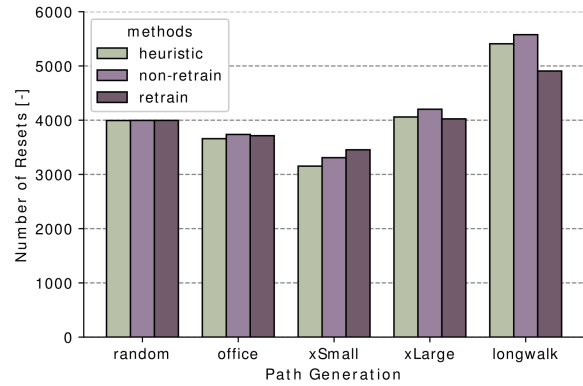


FIGURE 9: Number of Resets of Experiment 3

C. DISCUSSION

Environments with obstacles are more like a real environment than a square environment. Therefore, it can be said that the method that performs better in environments with obstacles is more versatile.

Our results show that the RL-based redirection controllers are advantageous in physical spaces with obstacles, as the number of resets is increasing at a much slower pace than that when using heuristic redirection controllers for increasing number of obstacles.

Even when the controller is not trained in an environment with obstacles, it somehow performs better than the heuristic controller, showing that the RL-based redirection controller has general versatility over different shapes of environments.

VIII. EXPERIMENT 3: LEARNING IN DIFFERENT WALKING PATHS

A. SIMULATION SETUP

We investigated how different walking paths affect the result of the RL-based redirection controller. Here, no obstacle was placed in the tracked place. We compared path-generating methods of *Exploration Small*, *Office*, *Exploration Large*, and *Long Walk* 2) describer in 4.3 by using the heuristic redirection controller, the RL redirection controller trained in the experiment 1, and the RL redirection controller retrained in the environment with various walking paths. We ran these controllers in a 100-km journey (one million simulation steps) for evaluating, and recorded the total count of reset procedure.

B. RESULTS

Fig 9 shows the total count of resets in the four different path generating algorithm conditions. As shown, the number of resets differs considerably in each path-generating algorithm. In comparison to heuristic, the RL method performs better in the Long Walk condition, slightly better in the Exploration Large condition, and worse in the Office and Exploration Small conditions.

C. DISCUSSION

As shown in Table 2 and Fig. 9, the number of resets increases when the average distance between targets increases. Further, we found out that the effectiveness of the RL-based redirection controller differs depending on the path-generating methods. Evaluated by the proportion to the heuristic redirection controller, the effectiveness in ascending order is as follows: Exploration (small), Office, Random, Exploration (large), Long Walk, which is also the average distance between targets in ascending order.

We assumed that the difference in the effectiveness is due to the average distance between targets, which may affect the efficiency of learning. As an evidence, the newly trained model in Exploration (small) is actually performed worse than the non-retrained model, which is an unexpected phenomenon. This requires further verification of the relevance between average distance and learning efficiency.

IX. GENERAL DISCUSSION

We determined that RL has general versatility and could perform better in environments with obstacles, compared with the heuristic method. The redirection controller using RL has the potential as a general redirection controller. Among the three redirection controllers with single component replaced by RL, the RL-curvature controller showed the best performance, which is almost the same as the heuristic one. There still exists room for improvement, such as replacing multiple components by RL. We take these improvements as our future work.

In the Experiment 2, the model trained in the obstacle free environment showed better results than the heuristic method in the obstacle environments. On the other hand, in the Experiment 3, some relearning models showed worse results than the trained models and heuristics. This shows that the proposed model has an environment suitable and not suitable for learning. There was a tendency for the number of resets to decrease as the distance between targets increased.

Moreover, we applied the output to the gain values; however, one can observe that the output value is very unstable.

Zhang et al. [38], [39] have investigated the influence of dynamically changing the translation and rotation gains and concluded that the oscillations of these gains lead to VR sickness and awareness of redirection operation. Therefore, it is suggested that the oscillation of the curvature gain also leads to VR sickness and awareness of redirection operation. We will evaluate these effects by further user tests. In our experiments, we set a negative reward for the vibration of the gain to solve this phenomenon; however, other measures may be considered, such as applying a filter to smooth the output. Another simple way to solve this problem is to decrease the decision frequency, which not only smooths the output value curve but also reduces the computation time, and it may lead to quality reduction.

One of the limitations is that you have to learning must be performed according to the environment, but the time required for one learning is approximately 2–3 h, which is less labor than manually adjusting the controller.

X. CONCLUSION

This paper presented a novel redirection controller using RL that can operate online. The proposed controllers can make an optimal plan without prior knowledge of the spatial composition of tracked spaces and VEs. Moreover, the proposed controller copes with obstacles placed in the real space.

We quantitatively evaluated heuristic and proposed redirection controllers through simulations in our experiments. In the preliminary experiments, we verified the most effective heuristic redirection controller in the physical spaces where obstacles are placed.

In the Experiment 1, the effectiveness of the redirection controller using RL was verified by applying RL to a part of the heuristic redirection controller. The results demonstrated that the redirection controllers were able to reduce the number of resets by up to 20.3% against the best heuristic controller. In addition, despite no prior knowledge, the RL controller showed a behavior similar to the S2C and Steer-to-Orbit. However, the output gains by RL oscillated in a short time.

In the Experiment 2, we confirmed the effectiveness of the proposed method in the environments with obstacles. Furthermore, in the experiment 3, we used multiple walking paths in VEs, and found that the number of resets decreases compared to when using the conventional general-purpose controller as the distance to the target is longer. These results suggested that the proposed method is effective when walking long distances in physical spaces with obstacles.

In the future, we will verify our method by considering real users from the view point of not only spatial efficacy but also cybersickness induced by redirection. In addition, we will examine the influence of the vibration of the curvature gains on the user. Furthermore, we will verify whether the proposed method is effective even when the obstacle moves, that is, when other players walk the same real space simultaneously.

APPENDIX A HYPERPARAMETER

The hyperparameter was tuned manually as in Table 5. Please check the ML-agents page⁴ for details of each parameter.

TABLE 5: Hyperparameter of PPO

parameter	value
batch size	2,048
buffer size	20,480
epsilon	0.2
gamma	0.995
number of layers	2
hidden units	128
lambda	0.995
learning rate	3×10^{-4}
max steps	1×10^6
memory size	256
num epoch	3
time horizon	256
sequence length	64

REFERENCES

- [1] S. Razzaque, D. Swapp, M. Slater, M. C. Whitton, and A. Steed, "Redirected walking in place," Proceedings of the workshop on Virtual environments, pp. 123–130, 2002. [Online]. Available: <http://dl.acm.org/citation.cfm?id=509709.509729>
- [2] N. Nilsson, T. Peck, G. Bruder, E. Hodgson, S. Serafin, E. Suma, M. Whitton, and F. Steinicke, "15 Years of Research on Redirected Walking in Immersive Virtual Environments," IEEE Computer Graphics and Applications, no. April, pp. 44–56, 2018.
- [3] E. Hodgson and E. Bachmann, "Comparing four approaches to generalized redirected walking: Simulation and live user data," IEEE Transactions on Visualization and Computer Graphics, vol. 19, no. 4, pp. 634–643, 2013.
- [4] E. Hodgson, E. Bachmann, and T. Thrash, "Performance of redirected walking algorithms in a constrained virtual world," IEEE Transactions on Visualization and Computer Graphics, vol. 20, no. 4, pp. 579–587, 2014.
- [5] M. A. Zmuda, J. L. Wonser, E. R. Bachmann, and E. Hodgson, "Optimizing constrained-environment redirected walking instructions using search techniques," IEEE Transactions on Visualization and Computer Graphics, vol. 19, no. 11, pp. 1872–1884, 2013.
- [6] T. Nescher, Y. Y. Huang, and A. Kunz, "Planning redirection techniques for optimal free walking experience using model predictive control," IEEE Symposium on 3D User Interfaces 2014, 3DUI 2014 - Proceedings, pp. 111–118, 2014.
- [7] D. Silver, T. Hubert, J. Schrittwieser, I. Antonoglou, M. Lai, A. Guez, M. Lanctot, L. Sifre, D. Kumaran, T. Graepel et al., "A general reinforcement learning algorithm that masters chess, shogi, and go through self-play," Science, vol. 362, no. 6419, pp. 1140–1144, 2018.
- [8] S. Gu, E. Holly, T. Lillicrap, and S. Levine, "Deep reinforcement learning for robotic manipulation with asynchronous off-policy updates," in 2017 IEEE international conference on robotics and automation (ICRA). IEEE, 2017, pp. 3389–3396.
- [9] A. E. Sallab, M. Abdou, E. Perot, and S. Yogamani, "Deep reinforcement learning framework for autonomous driving," Electronic Imaging, vol. 2017, no. 19, pp. 70–76, 2017.
- [10] E. A. Suma, G. Bruder, F. Steinicke, D. M. Krum, and M. Bolas, "A taxonomy for deploying redirection techniques in immersive virtual environments," Proceedings - IEEE Virtual Reality, pp. 43–46, 2012.
- [11] G. Bruder, F. Steinicke, K. H. Hinrichs, and M. Lappe, "Reorientation during body turns," in EGVE/ICAT/EuroVR, 2009, pp. 145–152.
- [12] F. Steinicke, G. Bruder, J. Jerald, H. Frenz, and M. Lappe, "Estimation of Detection Thresholds for Redirected Walking Techniques," IEEE Transactions on Visualization and Computer Graphics, vol. 16, no. 1, pp. 17–27, 2010. [Online]. Available: [papers2://publication/uuid/827DC4DE-CE85-40E0-B997-181D7EDBA5B1](https://publication/uuid/827DC4DE-CE85-40E0-B997-181D7EDBA5B1)

⁴<https://github.com/Unity-Technologies/ml-agents/blob/master/docs/Training-PPO.md>

- [13] T. Grechkin, J. Thomas, M. Azmandian, M. Bolas, and E. Suma, "Revisiting detection thresholds for redirected walking," *Proceedings of the ACM Symposium on Applied Perception - SAP '16*, pp. 113–120, 2016. [Online]. Available: <http://dl.acm.org/citation.cfm?doi=2931002.2931018>
- [14] E. Langbehn, P. Lubos, G. Bruder, and F. Steinicke, "Bending the Curve: Sensitivity to Bending of Curved Paths and Application in Room-Scale VR," *IEEE Transactions on Visualization and Computer Graphics*, vol. 23, no. 4, pp. 1349–1358, 2017.
- [15] B. Williams, G. Narasimham, B. Rump, T. P. McNamara, T. H. Carr, J. Rieser, and B. Bodenheimer, "Exploring large virtual environments with an HMD when physical space is limited," *Proceedings of the 4th symposium on Applied perception in graphics and visualization - APGV '07*, vol. 1, no. 212, p. 41, 2007. [Online]. Available: <http://portal.acm.org/citation.cfm?doi=1272582.1272590>
- [16] T. C. Peck, H. Fuchs, and M. C. Whitton, "Evaluation of reorientation techniques and distractors for walking in large virtual environments," *IEEE Transactions on Visualization and Computer Graphics*, vol. 15, no. 3, pp. 383–394, 2009.
- [17] S. Razzaque, *Redirected walking*. University of North Carolina at Chapel Hill, 2005.
- [18] M. Zank and A. Kunz, "Optimized graph extraction and locomotion prediction for redirected walking," *2017 IEEE Symposium on 3D User Interfaces, 3DUI 2017 - Proceedings*, pp. 120–129, 2017.
- [19] M. Azmandian, T. Grechkin, M. Bolas, and E. Suma, "Automated path prediction for redirected walking using navigation meshes," pp. 63–66, 2016.
- [20] H. Chen, S. Chen, and E. S. Rosenberg, "Redirected Walking Strategies in Irregularly Shaped and Dynamic Physical Environments," 2018. [Online]. Available: <http://wevr.adalsimeone.me/2018/WEVR2018{ }Chen.pdf>
- [21] Y. H. Cha, D. Y. Lee, and I. K. Lee, "Path Prediction Using LSTM Network for Redirected Walking," *25th IEEE Conference on Virtual Reality and 3D User Interfaces, VR 2018 - Proceedings*, pp. 527–528, 2018.
- [22] L. P. Kaelbling, M. L. Littman, and A. W. Moore, "Reinforcement learning: A survey," *Journal of artificial intelligence research*, vol. 4, pp. 237–285, 1996.
- [23] R. S. Sutton and A. G. Barto, *Reinforcement learning: An introduction*. MIT press, 2018.
- [24] C. J. Watkins and P. Dayan, "Q-learning," *Machine learning*, vol. 8, no. 3–4, pp. 279–292, 1992.
- [25] R. S. Sutton, D. A. McAllester, S. P. Singh, and Y. Mansour, "Policy gradient methods for reinforcement learning with function approximation," in *Advances in neural information processing systems*, 2000, pp. 1057–1063.
- [26] R. J. Williams, "Simple statistical gradient-following algorithms for connectionist reinforcement learning," *Machine learning*, vol. 8, no. 3–4, pp. 229–256, 1992.
- [27] V. R. Konda and J. N. Tsitsiklis, "Actor-critic algorithms," in *Advances in neural information processing systems*, 2000, pp. 1008–1014.
- [28] V. Mnih, A. P. Badia, M. Mirza, A. Graves, T. Lillicrap, T. Harley, D. Silver, and K. Kavukcuoglu, "Asynchronous methods for deep reinforcement learning," in *International conference on machine learning*, 2016, pp. 1928–1937.
- [29] J. Schulman, P. Moritz, S. Levine, M. Jordan, and P. Abbeel, "High-dimensional continuous control using generalized advantage estimation," *arXiv preprint arXiv:1506.02438*, 2015.
- [30] J. Schulman, F. Wolski, P. Dhariwal, A. Radford, and O. Klimov, "Proximal Policy Optimization Algorithms," 2017. [Online]. Available: <https://arxiv.org/pdf/1707.06347.pdf><http://arxiv.org/abs/1707.06347>
- [31] A. Juliani, V.-P. Berges, E. Vckay, Y. Gao, H. Henry, M. Mattar, and D. Lange, "Unity: A general platform for intelligent agents," *arXiv preprint arXiv:1809.02627*, 2018. [Online]. Available: <https://github.com/Unity-Technologies/ml-agents>
- [32] M. Azmandian, T. Grechkin, M. Bolas, and E. Suma, "Physical Space Requirements for Redirected Walking: How Size and Shape Affect Performance," in *ICAT-EGVE 2015 - International Conference on Artificial Reality and Telexistence and Eurographics Symposium on Virtual Environments*, M. Imura, P. Figueroa, and B. Mohler, Eds. The Eurographics Association, 2015.
- [33] M. Azmandian, T. Grechkin, M. Bolas, and E. Suma, "The redirected walking toolkit: a unified development platform for exploring large virtual environments," in *2016 IEEE 2nd Workshop on Everyday Virtual Reality (WEVR)*. IEEE, 2016, pp. 9–14.
- [34] F. Steinicke, G. Bruder, J. Jerald, H. Frenz, and M. Lappe, "Estimation of detection thresholds for redirected walking techniques," *IEEE transactions on visualization and computer graphics*, vol. 16, no. 1, pp. 17–27, 2010.
- [35] A. Nguyen and A. Kunz, "Discrete scene rotation during blinks and its effect on redirected walking algorithms," in *Proceedings of the 24th ACM Symposium on Virtual Reality Software and Technology*. ACM, 2018, p. 29.
- [36] T. C. Peck, H. Fuchs, and M. C. Whitton, "Improved redirection with distractors: A large-scale-real-walking locomotion interface and its effect on navigation in virtual environments," *Proceedings - IEEE Virtual Reality*, pp. 35–38, 2010.
- [37] E. Hodgson, E. Bachmann, and D. Waller, "Redirected walking to explore virtual environments: Assessing the potential for spatial interference," *ACM Transactions on Applied Perception (TAP)*, vol. 8, no. 4, p. 22, 2011.
- [38] R. Zhang, B. Li, and S. A. Kuhl, "Human sensitivity to dynamic translational gains in head-mounted displays," in *Proceedings of the 2nd ACM symposium on Spatial user interaction*. ACM, 2014, pp. 62–65.
- [39] R. Zhang and S. A. Kuhl, "Human sensitivity to dynamic rotation gains in head-mounted displays," in *Proceedings of the ACM Symposium on Applied Perception*. ACM, 2013, pp. 71–74.



YUCHEN CHANG is a master's student in the department of Mechano-Informatics at Graduate School of Information Science and Technology, The University of Tokyo. His research interests include redirected walking and machine learning.



KEIGO MATSUMOTO is a doctoral student in the department of Mechano-Informatics at Graduate School of Information Science and Technology, The University of Tokyo. His research interests include spatial perception, redirected walking, and visuo-haptic interaction. He is a student member of the ACM, IEEE and Virtual Reality Society of Japan (VRSJ). He received awards including Excellence Prizes in 20th Japan Media Arts Festival Entertainment Division, ICAT-EGVE 2017 Best Poster Award, SIGGRAPH ASIA 2017 E-tech Prize by Award Committee, President's award for Students of the University of Tokyo, and VRSJ Outstanding Paper Award in 24th Annual Meeting.



TAKUJI NARUMI is an associate professor at the Graduate School of Information Science and Technology, the University of Tokyo. His research interests broadly include perceptual modification and human augmentation with virtual reality and augmented reality technologies. He invented a novel haptic display, olfactory display, taste display and satiety display by utilizing cross-modal interactions. More recently, he also invented affective interface which evokes specific emotions through pseudo-generated body reactions. He received BE and ME degree from the University of Tokyo in 2006 and 2008 respectively. He also received his Ph.D. in Engineering from the University of Tokyo in 2011. He received awards including ACE 2014 Gold Paper Award, ICAT 2012 Best Paper Award, Augmented Human 2016 Third Best Paper Award, ACM SUI2015 Short paper honorable mention, and VRSJ Outstanding Paper Award.



TOMOHIRO TANIKAWA graduated at Graduate School of Engineering, the University of Tokyo (1998) and received the Ph.D (Engineering) from Graduate School of Engineering, the University of Tokyo (2001), focusing at image-based 3D reconstruction and rendering methods. His research interests include image-based rendering, interactive computer graphics, virtual reality and augmented reality. He has participated in a lot of international and national research and development projects and has developed image-based rendering algorithms to generate high quality images in real-time for the virtual environments and remote collaboration.



MICHITAKA HIROSE graduated at Graduate School of Engineering, the University of Tokyo (1979) and received the Doctor of Engineering from Graduate School of Engineering, the University of Tokyo (1982). His research interests include human interfaces, interactive computer graphics, wearable computers and virtual reality. He is in a position of leadership on Japanese virtual reality research community, and has been investigator of number of international and national research and development projects. For example, he was a project leader of Scalable Virtual Reality Project of TAO (Telecommunications Advancement Organization of Japan, is the predecessor of NICT) and developed a tele-immersion communication system which connects between CAVE-type immersive environments through the large-bandwidth gigabit communication network. He is a member of the ACM, IEEE and the former president of Virtual Reality Society of Japan (VRSJ).

...